Extremophiles (2018) 22:347–357
https://doi.org/10.1007/s00792-018-1002-2

ORIGINAL PAPER

Identification of a functional toxin–antitoxin system located in the genomic island PYG1 of piezophilic hyperthermophilic archaeon *Pyrococcus yayanosii*

Zhen Li[1,2] · Qinghao Song[1,2] · Yinzhao Wang[1,2] · Xiang Xiao[1,2] · Jun Xu[1,2]

Received: 21 September 2017 / Accepted: 23 December 2017 / Published online: 15 January 2018
© Springer Japan KK, part of Springer Nature 2018

Abstract
Toxin–antitoxin (TA) system is bacterial or archaeal genetic module consisting of toxin and antitoxin gene that be organized as a bicistronic operon. TA system could elicit programmed celldeath, which is supposed to play important roles for the survival of prokaryotic population under various physiological stress conditions. The phage abortive infection system (AbiE family) belongs to bacterial type IV TA system. However, no archaeal AbiE family TA system has been reported so far. In this study, a putative AbiE TA system (PygAT), which is located in a genomic island PYG1 in the chromosome of *Pyrococcus yayanosii* CH1, was identified and characterized. In *Escherichia coli*, overexpression of the toxin gene *pygT* inhibited its growth while the toxic effect can be suppressed by introducing the antitoxin gene *pygA* in the same cell. PygAT also enhances the stability of shuttle plasmids with archaeal plasmid replication protein Rep75 in *E. coli.* In *P. yayanosii*, disruption of antitoxin gene *pygA* cause a significantly growth delayed under high hydrostatic pressure (HHP). The antitoxin protein PygA can specifically bind to the PygAT promoter region and regulate the transcription of *pygT* gene in vivo. These results show that PygAT is a functional TA system in *P. yayanosii*, and also may play a role in the adaptation to HHP environment.

Keywords *Pyrococcus yayanosii* · Piezophilic hyperthermophile · Toxin–antitoxin system · Genomic island

Introduction

Toxin–antitoxin (TA) systems are widely spread in chromosomes and plasmids of bacteria and archaea (Goeders and Van Melderen 2014; Schuster and Bertram 2013; Yamaguchi et al. 2011). So far, TA systems have been categorized into six sub-classes (I–VI) based on the mechanisms of action and chemical nature of the antitoxin (Page and Peti 2016; Unterholzner et al. 2013). A typical TA system is composed of a toxin and antitoxin gene. Toxin gene always encodes a stable protein in all of the characterized bacterial TA systems, while the antitoxin gene is either protein (type II, IV, V and VI) or small non-coding RNAs (type I and III) (Schuster and Bertram 2013; Yamaguchi et al. 2011).

TA systems were firstly discovered on low copy plasmids as plasmid maintenance modules that were able to kill the daughter cells who failed to inherit the plasmids (Gerdes et al. 1986; Winther and Gerdes 2011). To date, some researchers believed that TA systems contribute to the adaptation of hosts under stress environments and the formation of persisted cells and biofilms (Wang and Wood 2011). In addition, TA systems also involve in stabilization of genomic islands (Bustamante et al. 2014) and selfish alleles (Ramisetty and Santhosh 2017), regulation of gene expression (Landini et al. 2014; Wang and Wood 2011) and programmed cell death (Hazan and Engelberg-Kulka 2004).

Moreover, there is mounting evidence showed that some TA elements can provide phage resistance, like Hok/Sok (Pecota and Wood 1996), MazEF (Hazan and Engelberg-Kulka 2004), RnlAB and LsoAB (Otsuka and Yonesaki

Communicated by L. Huang.

Electronic supplementary material The online version of this article (https://doi.org/10.1007/s00792-018-1002-2) contains supplementary material, which is available to authorized users.

✉ Jun Xu
xujunn@sjtu.edu.cn

[1] State Key Laboratory of Microbial Metabolism, School of Life Sciences and Biotechnology, Shanghai Jiao Tong University, Shanghai, China

[2] Institute of Oceanography, Shanghai Jiao Tong University, Shanghai, China

2012). The abortive infection (Abi) systems, for example, ToxIN of *Pectobacterium atrosepticum* and AbiE of *Lactococcus lactis* or *Streptococcus agalactiae*, have been shown to exert their function via toxin–antitoxin mechanism (Dy et al. 2014; Fineran et al. 2009).

AbiE of *L. lactis* consists of an antitoxin AbiEi and a toxin AbiEii, which are characterized by two conserved domains COG5340 and DUF1814, respectively. Such kind of two-component systems with COG5340-DUF1814 domains are found in 430 sequenced genomes of most major lineages of archaea and bacteria (Makarova et al. 2013). Homology of the DUF1814 domain also has been discovered in AbiG families (Makarova et al. 2013; O'Connor et al. 1999). It has been confirmed that GTP can specifically binds to the DUF1814 protein and appear to function as the toxin element, whereas the COG5340 protein that contains a predicted HTH domain is an antitoxin (Dy et al. 2014). AbiE system had been proved mostly located in many mobile genetic elements (MGEs) and plays a role in MGEs maintenance (Dy et al. 2014). In addition, AbiE of *L. lactis* provides resistance against the 936-type phage family by preventing DNA packaging (Tangney and Fitzgerald 2002).

AbiE system functions via a non-interacting (type IV) bacteriostatic TA mechanism. It has been assigned as an important representative in type IV TA system. The other members of the type IV TA system also have been identified, including YeeU–CbtA (Masuda et al. 2012a; Tan et al. 2011) and CptB–CptA (YafY/SdhE-YafX) (Masuda et al. 2012b) systems from *Escherichia coli*. Unlike AbiE, these groups of type IV TA system share the same feature to control polymerization of cytoskeletal proteins MreB and FtsZ.

TA systems have been extensively studied in bacteria, for example, at least 33 TA systems have been identified in *E. coli* (Yamaguchi et al. 2011). However, most of the studies on the TA system of archaea are based on bioinformatics analysis to identify mainly type II TA systems. RelBE and VapBC have been predicted as type II TA systems located in the mobile elements of Thermococcales and Methanococcales (Krupovic et al. 2013). Additionally, at least 26 TA gene loci (VapBC family) have been annotated in the genome of hyperthermophilic crenarchaeon *Sulfolobus solfataricus* (Cooper et al. 2009; Tachdjian and Kelly 2006). Global transcriptional analysis of *S. solfataricus* revealed that expression of several *vapBC* genes were triggered by the thermal shift from 80 to 90 °C, suggesting a role of TA system played in heat-shock response.

Pyrococcus yayanosii CH1 is a strictly piezophilic hyperthermophilic archaeon isolated from sample of 4100 m depth hydrothermal vent in the mid-Atlantic Ridge (Birrien et al. 2011; Jun et al. 2011; Zeng et al. 2009). The strain CH1 can grow within a temperature range of 80–108 °C and a pressure range of 20–120 MPa, with optima at 98 °C and 52 MPa, respectively (Zeng et al. 2009). In our previous study, a genomic island PYG1 of *P. yayanosii* was identified. Genetic analyses suggest that PYG1 could affect the host adaptation to the high temperature and HHP environments (Li et al. 2016b). Two genes in PYG1 encompass a pair of prokaryotic orthologous group families COG5340-DUF1814 (*PYCH_15320-PYCH_15330*), which showed high similarity to the corresponding region of a predicted genomic island in *T. barophilus* MP (Li et al. 2016b), formed a putative toxin–antitoxin system (PygAT) with AbiE conserved domains.

In this study, we showed that PygAT is a functional gene operon of *P. yayanosii* CH1 that could response to environment stress such as HHP. Either disruption of antitoxin gene *pygA* in *P. yayanosii* or overexpression of toxin gene *pygT* in *E. coli* could inhibit the growth of host.

Materials and methods

Strains, plasmids and culture conditions

Strains and plasmids used in this study are listed in Table 1. Bacterial growth was measured in a UV–VIS spectrophotometer at 600 nm (OD_{600}). *P. yayanosii* strains were cultivated in 100 ml serum bottles under anaerobic conditions at 95 °C and 0.1 MPa in 30 ml of TRM (Li et al. 2016b). After transformation, the strains were selected on TRM supplemented with 10 μM simvastatin (Sigma). Gelrite (1.5% w/v) was added to solidify the medium. The growth of archaea was monitored by cell counting using a Thomas chamber and light microscopy at a magnification of 40× (Li et al. 2016b; Zeng et al. 2009). Experiments were repeated in three biological replicates.

Bioinformatics analysis

Annotations of the gene function were confirmed by BLASTP analysis against NCBI database (https://www.ncbi.nlm.nih.gov/). Alignment of the amino acid sequences were performed using ClustalX2 and visualized by ESPript 3.0 (http://espript.ibcp.fr/ESPript/ESPript/). The second structure of proteins was analyzed using the web-based tool SWISS-MODEL (https://swissmodel.expasy.org/ interactive). The phylogenetic analysis was performed using the maximum likelihood phylogenetic tree algorithm with a software package for constructing evolutionary trees (MEGA, version 6.0).

Genetic manipulation and real-time quantitative PCR

Pyrococcus yayanosii A2 was transformed according to Li et al. (2016b). *P. yayanosii* A2 was cultivated in 50 ml

Table 1 Strains and plasmids used in the present study

Strains and plasmids	Description	References
Strains		
E. coli DH5α	*Escherichia coli* strain for gene cloning	Takara
E. coli BL21 (DE3)	*Escherichia coli* strain for protein expressing	TransGen Biotech
E. coli/pygT	The pET28a*/pygT* plasmid was transformed in *E. coli* BL21(DE3)	This study
E. coli/pygAT	The pET28a*/pygAT* plasmid was transformed in *E. coli* BL21(DE3)	This study
P. yayanosii A2	*pyrF* gene knockout strain of *P. yayanosii* A1	Li et al. (2015)
Δ*pygAT*	A mutant strain that the PYCH_15320-PYCH_15330 were replaced by a Sim^R cassette in *P. yayanosii* A2	This study
Δ*pygA*	A mutant strain that PYCH_15320 were replaced by a Sim^R cassette	This study
Δ*pygT*	A mutant strain that PYCH_15330 were replaced by a Sim^R cassette	This study
CΔ*pygA*	Δ*pygA* gene complement strain	This study
CΔ*pygT*	Δ*pygT* gene complement strain	This study
Plasmids		
pLMO12102	pGT5 replication area of *P. abysii* GE5 which contains *sso*, *dso*, Rep75 protein were inserted in pUC19 plasmid of *E. coli*	Lab stock
pLMO12103	pGT5 replication area of *P. abysii* GE5 which contains *sso*, *dso*, Rep75 protein and Sim^R cassette were inserted in pUC19 plasmid of *E. coli*	Lab stock
pLMO12103/*pygAT*	*pygAT* was cloned into the plasmid pLMO12103	This study
pLMO04	Derivative of pLMO03, without Sim^R cassette	(Li et al. 2016b)
pLMO04Δ*pygA*	Homologous recombination suicide vector for *pygA* knockout	This study
pLMO04Δ*pygT*	Homologous recombination suicide vector for *pygT* knockout	This study
pLMO04Δ*pygAT*	Homologous recombination suicide vector for *pygAT* knockout	This study
pUC19	Clone vector	Lab stock
pUC19/*pygAT*	*pygAT* was cloned into the clone vector pUC19	This study
pET28a	Expression vector	Lab stock
pET28a/*pygAT*	Clone *pygAT* operon into the specific site of pET28a which was digested by *Nde* I/*Sal* I	This study
pET28a/*pygA*	Clone *pygA* into the specific site of pET28a which was digested by *Nde* I/*Sal* I	This study
pET28a/*pygT*	Clone *pygT* into the specific site of pET28a which was digested by *Nde* I/*Sal* I	This study

TRM medium at 95 °C, 0.1 MPa for 12 h, and cells in the late exponential growth phase were harvested and subsequently resuspended in 200 µl of cold transformation buffer (80 mM $CaCl_2$). The suspended cells were incubated on ice for 0.5 h under anaerobic conditions, and subsequently 3 µg homologous recombinant suicide plasmids were added to the suspension and incubated on ice for 1 h. After heat shock at 95 °C for 45 s, the suspension was incubated on ice for 10 min. The treated suspension was transferred to 8 ml of TRM medium (without simvastatin) and cultured for two generations. The culture was spread onto TRM solid medium supplemented with 10 µM simvastatin and further incubated for 3–5 days at 95 °C. Transformants were verified by PCR amplification. Subsequently, the native transformant was counter selected by 5-FOA. The resulting mutant was confirmed by PCR amplification.

The genomic DNA from *P. yayanosii* was extracted as previously reported (Li et al. 2015). The total RNA of *P. yayanosii* was extracted by Trizol. RNA purification was performed with DNase I (Thermo). The cDNA was prepared using a cDNA synthesis kit (Thermo). Plasmids were extracted from *E. coli* DH5α using the plasmid extraction kit (Omega). The DNA purification was conducted using a DNA gel extraction kit or the Cycle-Pure Kit (Omega). The restriction endonucleases and T4 ligase were purchased from Takara or NEB. DNA sequencing and oligonucleotide synthesis were performed at Sangon (Sangon Biotech). Real-time quantitative PCR was carried out with an ABI 7500 system. 16S rRNA gene was used as an internal standard. The $2^{-\Delta\Delta CT}$ method was used to analyze the relative gene expression.

Culturing experiments under HHP

The procedure of HHP culturing experiments is consistent with that described previously (Li et al. 2016b). All manipulations before the pressurized culturing experiments were performed anaerobically inside an anaerobic glove box (Coy Lab). Cultivation of *P. yayanosii* was performed using a custom-built high-pressure/high-temperature incubation system. A 10-ml plastic syringe was used as the container of liquid medium. After inoculation, the needle head of the syringe

was sealed tightly with a butyl rubber stopper. The syringe was then placed inside a titanium chamber that was pressurized to the appropriate hydrostatic pressure and maintained at high temperature.

Toxicity and antitoxicity assays

The putative toxin gene *pygT* and *pygA–pygT* gene pairs were amplified using primers listed in Supplementary Table 1. The products were cloned into pET28a and the resulting recombinants were transformed into *E. coli* BL21. *E. coli* were cultured in 20 ml LB with 50 μg/ml kanamycin at 37 °C. When the OD_{600} reached to about 0.8, 50 μl bacteria solution of different dilutions were inoculated on the LBA plates which contain or not contain inducer IPTG (final concentration 0.5 mM), respectively. These LBA plates were incubated overnight at 37 °C. Moreover, IPTG was also added to the remaining culture medium to induce toxin expression. 100 μl bacteria solution were diluted with phosphate-saline buffer (PBS) and spread onto the LBA plates to determine the number of colony-forming units (CFU/ml) every 2 h from OD_{600} reached to about 0.4.

Plasmid stability assays

Recombinant plasmids pUC19/*pygAT* and pLMO12103/*pygAT* contain the PygAT system were constructed. An *E. coli* plasmid pUC19 and *P. yayanosii–E. coli* shuttle plasmids pLMO12102 and pLMO12103 were control groups, respectively. These plasmids were transformed into *E. coli* DH5a and cultured in LB medium without any antibiotics at 37 °C and 200 rpm for 24 h. The above strains were serially sub-cultured for 5 days, and each day of bacterial solution was diluted and spread on antibiotics-free plate. About 100 colonies were randomly selected to replica on plates containing antibiotics to determine the plasmids maintenance.

Protein expression and purification

Escherichia coli BL21 (DE3) strain harboring pET28a/*pygA* plasmid was cultivated in 1 l of Luria–Bertani (LB) medium supplemented with 50 μg/ml kanamycin at 37 °C for 4 h. When the OD_{600} reached about 1.0, expression of the protein His_6-PygA was induced with 0.5 mM isopropyl-*b*-D-thiogalacto-pyranoside (IPTG) and the culture was cultivated overnight at 16 °C, 200 rpm. Cells were harvested by centrifugation at 8000×*g* for 10 min at 4 °C. The cell pellet was resuspended in 25 ml lysis buffer (20 mM Tris–HCl, 300 mM NaCl, 10% glycerol, pH 8.0) and sonicated on ice for 30 min. Then, cells were centrifuged by centrifugation at 10,000×*g* for 30 min at 4 °C. Collect the supernatant and place it in a column containing 1 ml of Ni Sepharose High Performance resin (GE Healthcare). Unbound proteins were removed through washing three times with 10 ml of the wash buffer (20 mM Tris–HCl, 300 mM NaCl, 10% glycerol, 20 mM imidazole, pH 8.0). Protein His_6-PygA was eluted with elution buffer (20 mM Tris–HCl, 300 mM NaCl, 10% glycerol, 300 mM imidazole, pH 8.0). Proteins were dialysed overnight with 20 mM Tris–HCl, 300 mM NaCl, 50% glycerol. The purified protein was stored at − 20 °C and its concentration was determined by the Bradford method (Sangon Biotech). 12% SDS-PAGE was used to confirm the purity of protein.

Electrophoretic mobility shift assay (EMSA)

The putative promoter region of *pygAT* was amplified with specific primers (From upstream 226 bp of the initiation codon ATG to the downstream 22 bp of it.) and purified with Cycle Pure kit (Omega). The EMSA reaction system (20 μl) is as follows: 0.5 μl DNA was incubated with different amounts of protein His_6-PygA in 4 μl EMSA buffer (100 mM HEPES, pH 7.5; 5 mM EDTA; 5 mM DTT and 1% w/v Tween 20,150 mM KCl), 1 μl Poly d[I-C] and 13.5 μl ddH_2O at room temperature for 20 min. The mixtures were then loaded onto 6% native polyacrylamide gel electrophoresis at 100 V for 1 h at room temperature and then the gel was stained with GelRed.

DNase I footprinting assay

DNA probe which contains *pygAT* promoter region was amplified with FAM-labeled primers (He et al. 2015; Li et al. 2016a). The reaction system was the same as EMSA experiment. The mixture was treated with 0.02 units of DNase I (ThermoFisher) at room temperature for 10 min. The reaction was stopped by adding 0.25 μl 0.5 M EDTA and incubating in a water bath at 75 °C for 15 min. Then, the treated DNA was purified and mixed with GeneScan-LIZ500 size standard, assayed with Applied Biosystems 3730XL DNA analyzer (identified by Sangon Biotech) (He et al. 2015; Li et al. 2016a). Electropherograms were analyzed using the GeneMarker software. Protein binding sites were determined by analyzing the decrease of peaks after binding of different concentrations of proteins to DNA.

Results

A putative TA system was identified in the genomic island PYG1 of *P. yayanosii*

In the genomic island PYG1, a putative TA system was identified as a bicistronic operon based on the blast search of the conserved domains (COG5340-DUF1814) against

NCBI database. PygA (PYCH_15320) possess a winged helix-turn-helix (wHTH) domain of AbiEi-related protein (Aravind et al. 2005; Dy et al. 2014), and it has a predicted secondary structure of H1-S1-H2-t-H3-S2-W1-S3-W2 (H = helix. S = strand, and W = Wing) that represent of typical antitoxin protein (Fig. 1a). Multiple sequence alignment of the putative toxin protein PygT (PYCH_15330) revealed that the enzyme shared four conserved motifs with other homologs that belongs to the AbiEii family from different sources (archaea and bacteria) (Fig. 1b). Either antitoxin protein PygA or toxin protein PygT exhibit low sequence identity (11.15 and 17.36%, respectively) to the antitoxin protein AbiEi (Accession no. WP_012477749.1) and the toxin protein AbiEii (Accession no. WP_012477748.1) of *Lactococcus lactis* (Fig. S1). The phylogenetic analysis of PygA and PygT shows that they are located in a different branch compared with their counterparts from bacteria (Fig. S2).

pygA and *pygT* were organized into an operon

In PYG1, the putative toxin gene *pygT* overlap with its upstream antitoxin gene *pygA* by 11 nucleotides, and were separated by a 13 bp region with PYCH_15340 (Fig. 2a). Amino acid sequence of PYCH_15340 shared 93% identity with the N-terminal end of a putative protein TERMP_01870 of *Thermococcus barophilus* MP (Accession no. WP_013468141.1). TERMP_01870 and PygT have 95% amino acid sequence identity.

Using reverse transcripted total RNA of *P. yayanosii* as templates, cDNAs were amplified by specific primers to analyze whether the putative TA loci gene pairs were co-transcribed or not (Fig. 2a). A band with the expected size was obtained for *pygA–pygT* (Fig. 2b), but not for *pygT*-PYCH_15340 (Fig. 2c). Genomic DNA and RNA also were used to amplify as positive and negative controls, respectively. These results suggested that *pygAT* was organized into an operon.

pygA and *pygT* constitute a functional toxin–antitoxin module

Recombinant expression plasmids pET28a/*pygT* and pET28a/*pygAT* were transformed into *E. coli* BL21 (DE3) to verify that the PygAT is a functional TA system. The assumed toxin gene *pygT* was overexpressed and can inhibit cell growth after IPTG induction (Fig. 3a). Whereas, strains that contained a complete PygAT system or only contained empty vector pET28a did not inhibit cell growth (Fig. 3a). Meanwhile, the normal growth also was observed without

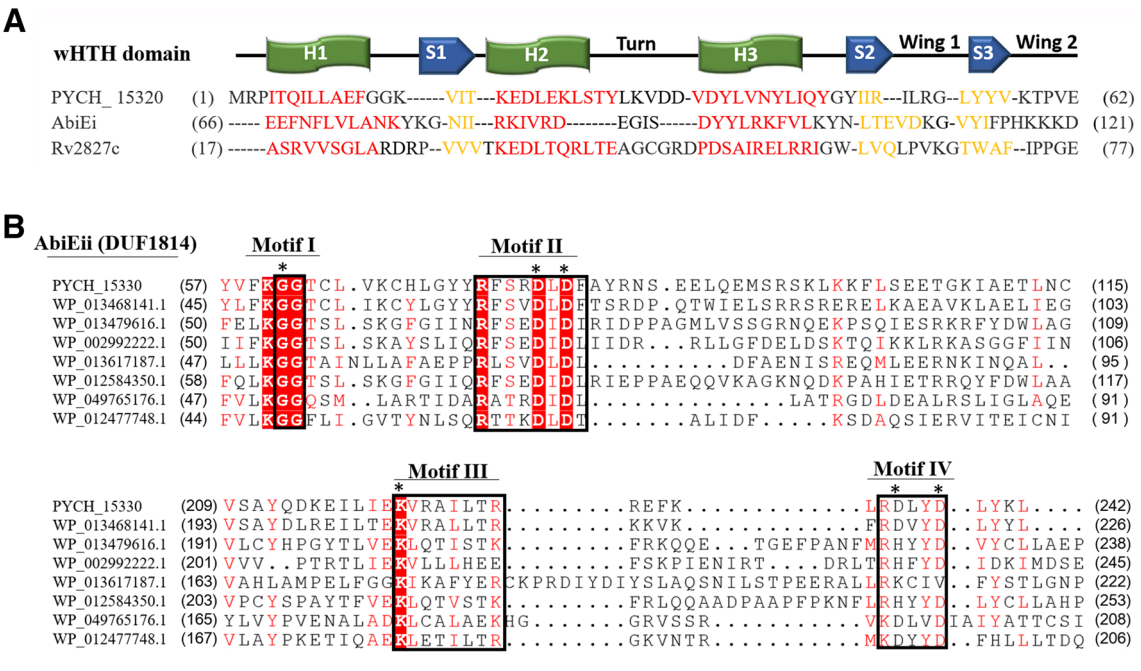

Fig. 1 Schematic diagram of conserved domains COG5340-DUF1814 of PygAT **a** PYCH_15320 sharing a wHTH domain with AbiEi (Accession no. WP_012477749.1) of *Lactococcus lactis* and Rv2827c (Accession no. NC_000962.3) of *Mycobacterium tuberculosis*. **b** Multiple amino acid sequence alignment of PYCH_15330 with homologs showing four motifs (I–IV). WP_013468141.1: hypothetical protein from *Thermococcus barophilus* MP; WP_013479616.1: hypothetical protein from *Asticcacaulis excentricus*; WP_002992222.1: hypothetical protein from *Myroides odoratus*; WP_013617187.1: hypothetical protein from *Bacteroides salanitronis*; WP_012584350.1: hypothetical protein from *Thauera* sp. MZ1T; WP_049765176.1: hypothetical protein from *Olsenella uli*; WP_012477748.1: AbiEii from *Lactococcus lactis*. Black boxes represent motifs

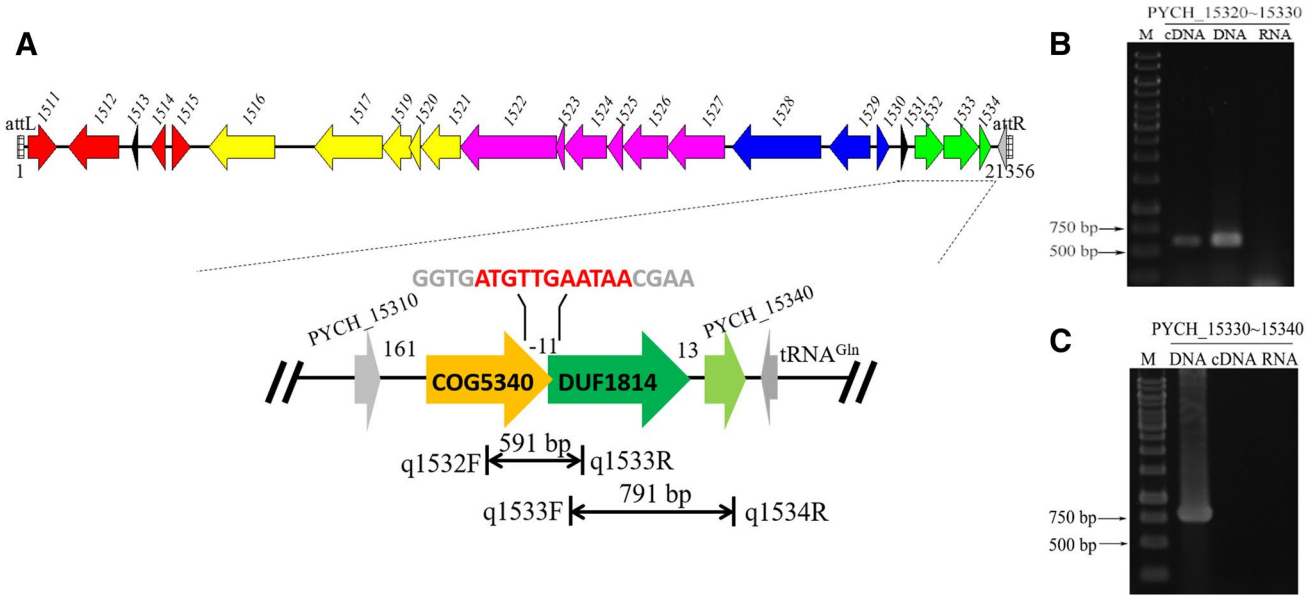

Fig. 2 Co-transcription analysis of *pygAT* operon in the *P. yayanosii* genome. **a** Schematic diagram of the bicistronic structure of *pygAT*. **b** Confirmation of the co-transcript of *pygA* and *pygT* using primers q1532F/q1533R and **c** primers q1533F/q1534R

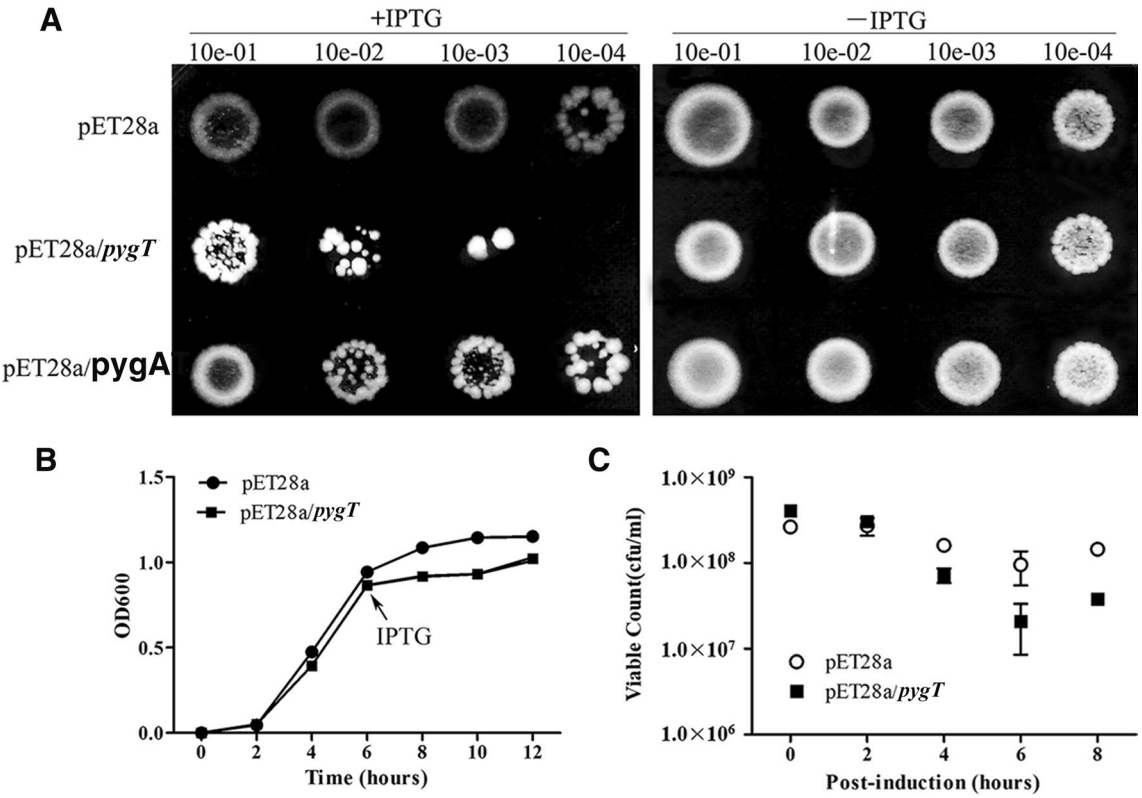

Fig. 3 Toxic effect of PygT on the growth of *E. coli* BL21 (DE3). **a** Overexpression of *pygT* inhibited cell growth. Plasmids pET28a and pET28a/*pygAT* were control groups in this experiment. **b** Strains which contain plasmids pET28a and pET28a/*pygT* were cultured in liquid LB medium and the toxin gene *pygT* was induced by IPTG at OD_{600} = 0.8. **c** Bacteria was diluted and coated on the LBA plates containing ampicillin resistance and then was counted on the flat plate. Data shown are mean ± SD of three biological replicates

IPTG induction. Then, the strains that transformed with pET28a and pET28a/*pygT* plasmids were cultured in liquid LB medium. We found that the growth of cells was inhibited after the toxin gene *pygT* was induced by IPTG at $OD_{600} = 0.8$ (Fig. 3b). In addition, when the OD_{600} reached to about 0.4, the bacteria was diluted and coated on the LBA plates containing ampicillin resistance, we can see that the number of bacterial colonies overexpressed the toxin gene *pygT* was lower than that of the control group (Fig. 3c). The results above suggested that PygAT is a functional toxin–antitoxin module.

PygAT plays a role in maintaining *P. yayanosii–E. coli* shuttle plasmids in *E. coli*

The AbiE family TA systems usually present in mobile genetic elements (MGEs), such as plasmids or genomic islands, and almost all types of TA systems have the ability to stabilize the extrachromosomal genetic elements. To test whether the PygAT system can also provide stabilization for MGEs, we transformed several recombinant plasmids pLMO12103/*pygAT* and pUC19/*pygAT* (including PygAT) into *E. coli* (DH5a). An *E. coli* plasmid pUC19 and *P. yayanosii–E. coli* shuttle plasmids pLMO12102 and pLMO12103 were control groups, respectively. The transformants were cultured in liquid LB medium without any antibiotics. After 5 days, the survival rates of the two strains were calculated by colony counting method on the LBA plates with ampicillin resistance. We found that the numbers of the strain carrying pLMO12102 and pLMO12103 plasmids declined sharply after successive transfer culturing on the LBA plate with ampicillin resistance. The survival rate on the fifth day was only about 0.625–2.2%, while strains carrying pLMO12103/*pygAT*, pUC19/*pygAT* and pUC19 plasmids in LBA plate did not affect the survival ability (Fig. 4). Shuttle plasmid pLMO2102 was constructed on the basis of pUC19 by adding the *P. abyssi* plasmid pGT5 replication protein Rep75. These results indicated that PygAT system plays a crucial role in maintaining of *P. yayanosii–E. coli* shuttle plasmids containing archaeal plasmid replication protein in *E. coli*.

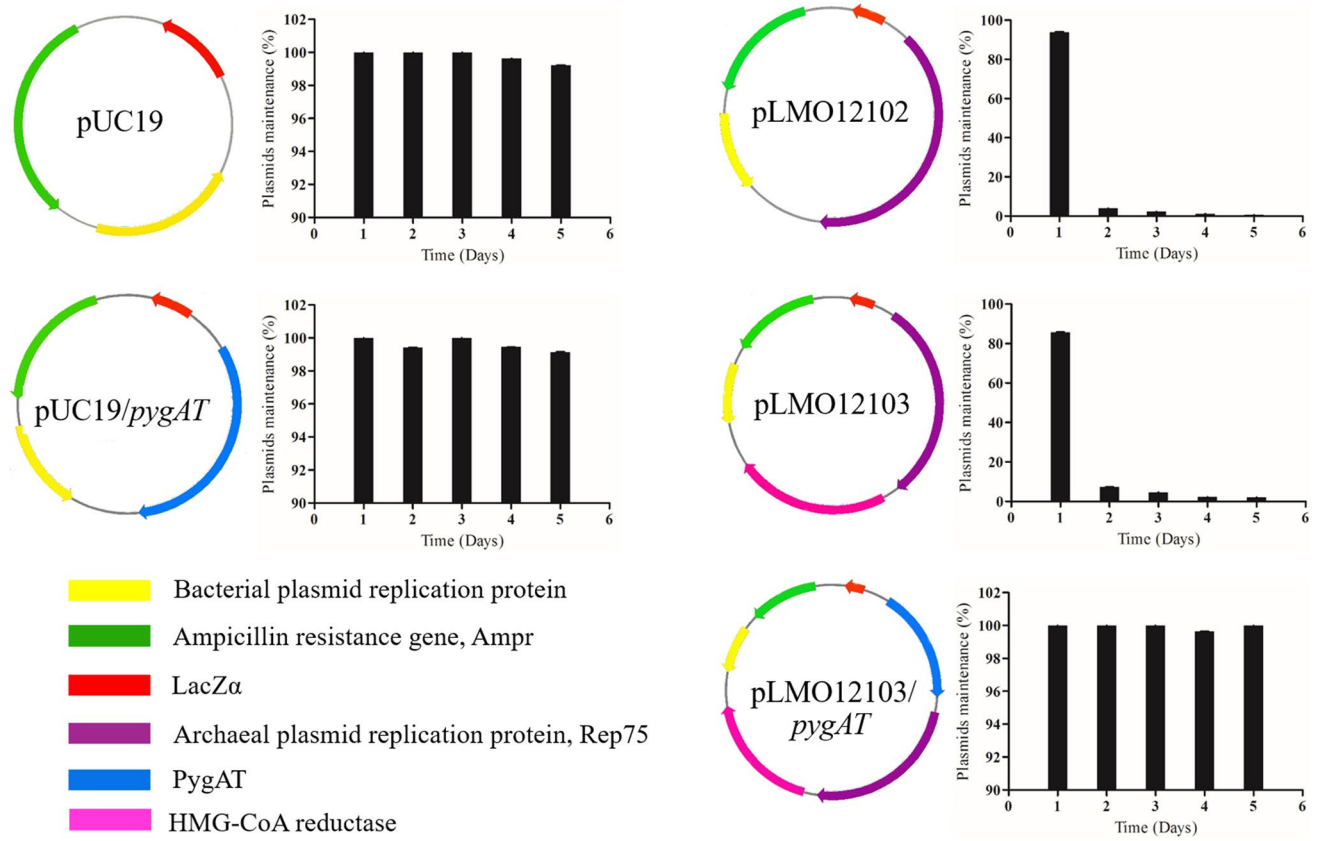

Fig. 4 PygAT improved *P. yayanosii–E. coli* shuttle plasmid stability. *E. coli* DH5α carrying plasmids with and without the PygAT operon (pLMO12103/*pygAT*, pUC19/*pygAT* and pLMO12102, pLMO12103 and pUC19, respectively) were used to verify the plasmid stability without antibiotic selection. Ratio of plasmids maintenance was calculated by counting the difference in colony numbers between replica plates containing or not containing antibiotics

PygT affects HHP adaptation of *P. yayanosii*

We constructed several gene knockout mutant strains of *P. yayanosii* including Δ*pygT*, Δ*pygA* and Δ*pygAT* to evaluate the physiological function of PygAT system. These strains were cultured at 0.1, 52 MPa (the optimum pressure) and 80 MPa. The growth curves of strains showed that there were no significant differences between the mutant and the parent strains at 0.1 MPa (Fig. 5a). However, comparing 52 and 80 MPa, we found that the lag phase of mutant strain Δ*pygA* was significantly prolonged. The mutant strain Δ*pygA* entered the logarithmic growth phase after growing 16 h (52 MPa) or 24 h (80 MPa). The gene complementary strain CΔ*pygA* was constructed and the growth of the strain was recovered to wild type (Fig. 5b, c). We analyzed the transcription level of *pygT* gene in wild strain A2, mutant strain Δ*pygA* and complementary strain CΔ*pygA* under 0.1 and 52 MPa. The results showed that the transcription level of *pygT* was derepressed in Δ*pygA* when the antitoxin was missing, while the transcription level of *pygT* was repressed in CΔ*pygA* when the antitoxin was complemented (Fig. 5d). These data confirmed that the transcription of *pygT* could respond to HHP stress in *P. yayanosii*, and the antitoxin gene *pygA* can regulate the expression of *pygT* in vivo.

PygA specifically binds to two regions in the promoter of the *pygAT* operon

EMSA was performed to assess the direct interaction of the His_6-PygA protein (Fig. S3) with *pygAT* operon promoter region. In reaction system, the promoter DNA showed obvious blockage with the increase of His_6-PygA protein concentration, while no blocking was observed in the control groups (Fig. 6a). Furthermore, DNase I footprinting technique was used to identify the exact banding sites of His_6-PygA protein in promoter region. We found that the

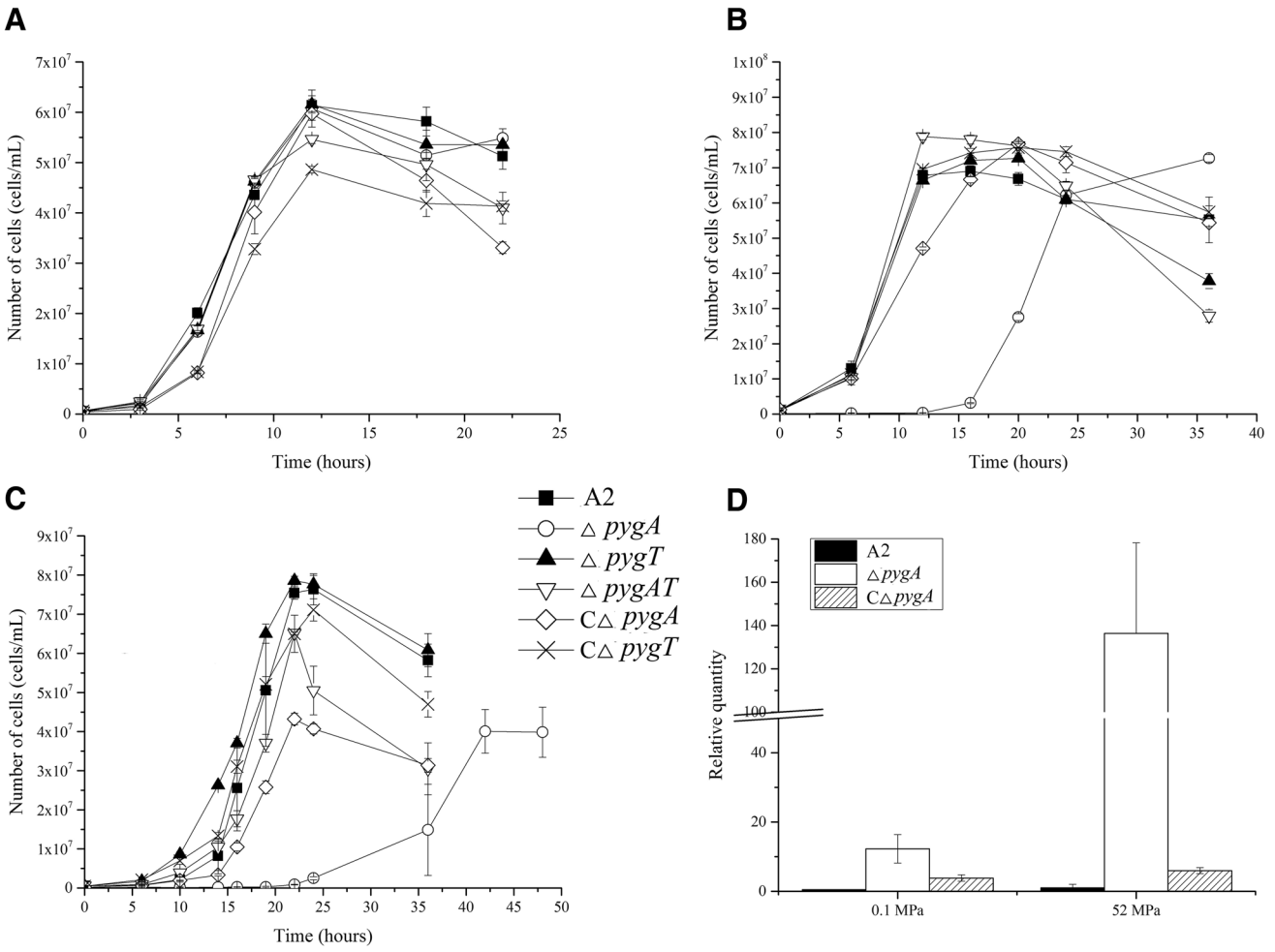

Fig. 5 PygAT affected the growth of *P. yayanosii* under different hydrostatic press conditions. The growth curves of *P. yayanosii* strains (A2, Δ*pygA*, Δ*pygT*, Δ*pygAT*, CΔ*pygA*, CΔ*pygT*) under **a** 0.1 MPa, **b** 52 MPa and **c** 80 MPa. **d** Transcription levels of *pygT* gene in (A2, Δ*pygA*, CΔ*pygA*) under 0.1 and 52 MPa

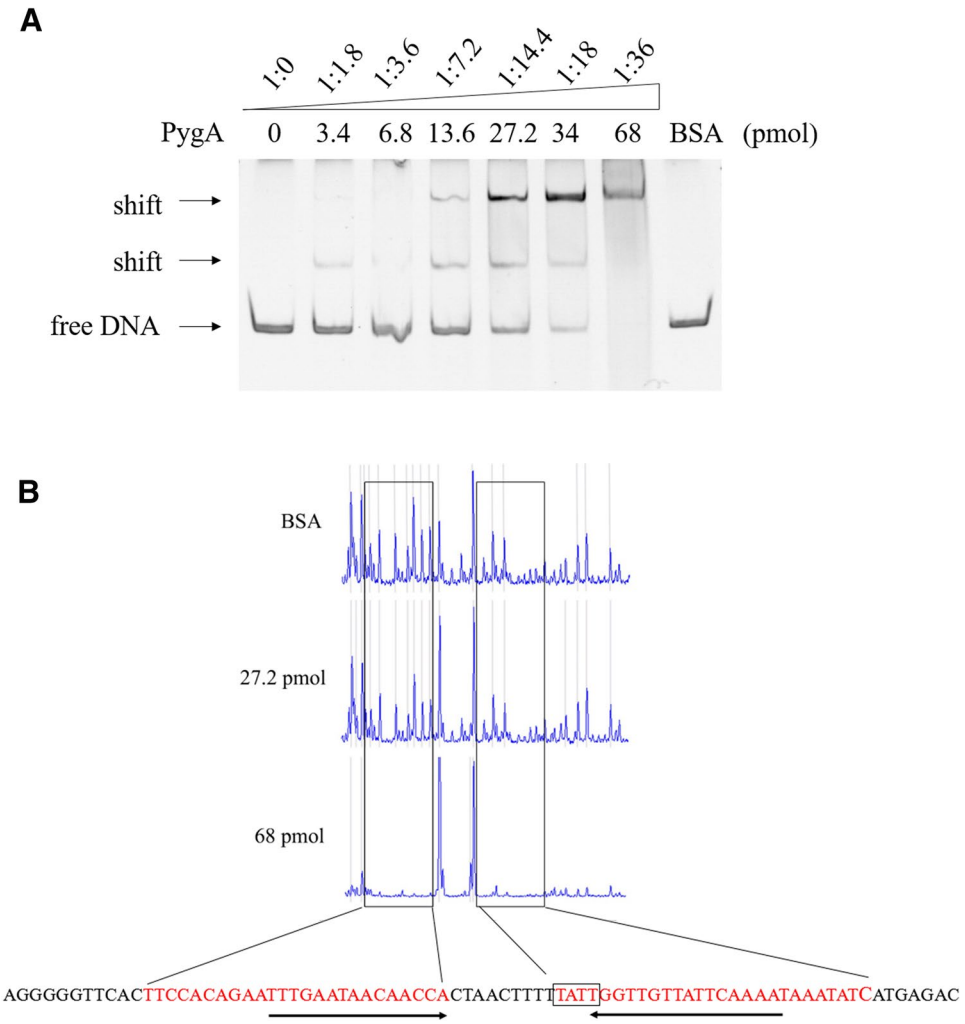

Fig. 6 Antitoxin protein PygA specifically binds to the putative PygAT promoter region. **a** EMSA experiment was performed to verify the binding of PygA protein (from 0 to 68 pmol) with the putative promoter DNA. **b** DNase I footprinting assay on the binding site of PygA and promoter region. Black arrows represent a pair of palindrome sequences (TTTGAATAACAACCA and TGGTTGTTATTCAAA). Black box (TATT) was predicted as a putative TATA-box

peaks of two regions decreased or disappeared after binding to DNA with different concentrations of protein. It suggested that these two regions in the *pygAT* operon promoter were apparently protected by His_6-PygA protein. We also found a pair of palindromes (TTTGAATAACAACCA and TGG TTGTTATTCAAA) in these two regions (Fig. 6b). All these results suggested that the antitoxin gene *pygA* can regulate the expression of *pygT* through specifically banding to the promoter region of *pygAT* operon.

Discussion

The AbiE family was firstly recognized as a pair of genes with COG5340-DUF1814 conserved domains (Garvey et al. 1995) and has been assigned as type IV TA system in several bacteria, such as *L. lactis* and *S. agalactiae* (Dy et al. 2014). To date, the understanding of the bacterial AbiE TA system is still very limited and almost there is no information of archaeal AbiE TA system.

There are 11 potential TA loci in the genome of *P. yayanosii* CH1 as predicted by a toxin–antitoxin database TADB (Shao et al. 2011). The putative TA system PygAT we studied here was not included in TADB but was found by a Blast search. Although the sequence homolog between PygAT on the genomic island PYG1 of *P. yayanosii* to conserved domains of AbiE family proteins of *L. lactis* was relative low, it provides good opportunity to study the archaeal counterparts in a phylogenetic point of view of type IV TA systems.

Our experiments indicated that the putative PygAT system can work as a functional TA module in *E. coli*. Interestingly, the toxin showed slight inhibition effect when the strains were cultured in liquid medium. This phenomenon is similar to the results of previous study by Dy et al. (2014). Research on the AbiE system of *L. lactis* also has been verified that it is a reversible bacteriostatic TA system. Four hours after the AbiEii was induced, the cells could be restored to the initial cell numbers (Dy et al. 2014). These results indicate that the inhibition of the toxin on the

growth of the bacteria could not be a lethal effect, but a stress response in the face of external stimulus.

The MosAT system located in the *Vibrio cholera* SXT ICE can promote the genomic island maintenance, which has a conserved domain COG2253-COG5340 similar to AbiE (Wozniak and Waldor 2009). Although we have no direct evidence to prove the effect of PygAT on the stability of the genomic island, but we have confirmed that PygAT enhances the genetic stability of shuttle plasmid carrying archaeal plasmid replication protein Rep75 in *E. coli*. PygAT has a close homologue, i.e., TbgAT, which is also located in a genomic island TBG1 of *T. barophilus* MP (Li et al. 2016b). We assume that the presence of the either PygAT or TbgAT contributes to the stabilization of the genomic islands PYG1 and TBG1 in these two piezophilic archaeon, respectively.

To find whether there is a relationship between physiological function of PygAT and HHP stress in *P. yayanosii*, we constructed a series of gene knockout mutants, and measured their growth curves under different pressure conditions. We found that the lag phase of mutant strain Δ*pygA* was significantly prolonged with the pressure was improved to 52 and 80 MPa. The transcription level of toxin gene *pygT* was significantly up-regulated in Δ*pygA* strain. Subsequently, the EMSA and DNase I footprinting experiments confirmed that PygA can regulate the expression level of *pygT* in *P. yayanosii* by interacting with two DNA regions of in the promoter region of *pygAT* operon. These results indicated that regulation on PygAT is part of the adaptation to HHP stress response in *P. yayanosii*.

In bacteria, type II TA system MqsR/MqsA regulate the general stress response (GSR). The GSR allows cells to survive long periods of starvation and environmental stresses. And it is accompanied by a significantly reduced growth rate, and it appears that TA systems are the means by which growth is slowed. Specifically, during stress, Lon protease degrades MqsA, which leads to induction of the stress regulating factor RpoS in *E. coli*, which in turn increases the concentration of the second messenger 3,5-cyclic diguanylic acid (c-di-GMP), inhibits motility and increases cell adhesion and biofilm formation (Wang et al. 2011). Moreover, AbiEii (DUF1814) of *L. lactis* functions as a nucleoside transferase (NTase) belong to the DNA polyβ superfamily, which can specifically bind GTP and transfer nucleotide to an unknown target (Dy et al. 2014). In our study, we found that PygT can specifically bind GTP when purified PygT was incubated with 5′-FAM labeled GTP and ATP (Fig. S4). According to these, we suspect that the antitoxin is deleted when the cells in high pressure uninhibited toxin PygT transferred nucleotides as a signaling molecule to the target, and further affects the biological processes that are significantly affected by the effect of pressure.

A lot of processes like transporters, motility and respiratory chain components, directly related to the membrane composition are also affected by HHP in piezophiles (Simonato et al. 2006). In *P. yayanosii* CH1, the biological processes that are significantly affected by the effect of pressure may involve in translation, chemotaxis, energy metabolism (hydrogenases and formate metabolism) and CRISPR sequences associated with cellular apoptosis susceptibility proteins (Michoud and Jebbar 2016). Meanwhile, due to the potential substrate diversity of NTase, it is difficult to accurately predict the toxin protein substrate. Therefore, to explain the mechanism of the phenomenon of Δ*pygA* under high pressure, it is necessary to do further research.

Meanwhile, the very low biomass and metabolic activity during the lag phase of the bacterial or archaeal growth cycle also resulted in a very limited understanding of this stage (Rolfe et al. 2012). CbtA is a toxin gene of type IV TA system YeeU–CbtA which can inhibit the polymerization of bacterial cytoskeletal proteins (MreB and FtsZ) and influence the shape of cells (Masuda et al. 2012a; Tan et al. 2011). We found the cell morphology of the mutant strains (Δ*pygA*, Δ*pygT* and Δ*pygAT*) did not change significantly (Fig. S5).

In conclusion, we reported a functional AbiE family TA system PygAT that located on the genomic island PYG1 of *P. yayanosii*. This is the first archaeal example of a type IV TA system, in which both physiological functions of stabilizing plasmid and participating in HHP stress response were suggested.

Author contributions ZL XX and JX designed the experiments; ZL and QHS performed the experiments; ZL, YZW and JX drafted the manuscript. All authors discussed and reviewed the manuscript.

Funding This study was supported by the National Natural Science Foundation of China (41676121, 41376137) and the National Basic Research Program of China ("973" Program 2014CB441503).

References

Aravind L, Anantharaman V, Balaji S, Babu MM, Iyer LM (2005) The many faces of the helix-turn-helix domain: transcription regulation and beyond. FEMS Microbiol Rev 29:231–262

Birrien JL, Zeng X, Jebbar M, Cambon-Bonavita MA, Querellou J, Oger P, Bienvenu N, Xiao X, Prieur D (2011) *Pyrococcus yayanosii* sp. nov., an obligate piezophilic hyperthermophilic archaeon isolated from a deep-sea hydrothermal vent. Int J Syst Evol Microbiol 61:2827–2831

Bustamante P, Tello M, Orellana O (2014) Toxin–antitoxin systems in the mobile genome of *Acidithiobacillus ferrooxidans*. PLoS One 9:e112226

Cooper CR, Daugherty AJ, Tachdjian S, Blum PH, Kelly RM (2009) Role of vapBC toxin–antitoxin loci in the thermal stress response of *Sulfolobus solfataricus*. Biochem Soc Trans 37:123–126

Dy RL, Przybilski R, Semeijn K, Salmond GP, Fineran PC (2014) A widespread bacteriophage abortive infection system functions through a type IV toxin–antitoxin mechanism. Nucleic Acids Res 42:4590–4605

Fineran PC, Blower TR, Foulds IJ, Humphreys DP, Lilley KS, Salmond GP (2009) The phage abortive infection system, ToxIN, functions as a protein-RNA toxin–antitoxin pair. Proc Natl Acad Sci USA 106:894–899

Garvey P, Fitzgerald GF, Hill C (1995) Cloning and DNA sequence analysis of two abortive infection phage resistance determinants from the lactococcal plasmid pNP40. Appl Environ Microbiol 61:4321–4328

Gerdes K, Rasmussen PB, Molin S (1986) Unique type of plasmid maintenance function: postsegregational killing of plasmid-free cells. Proc Natl Acad Sci USA 83:3116–3120

Goeders N, Van Melderen L (2014) Toxin–antitoxin systems as multilevel interaction systems. Toxins (Basel) 6:304–324

Hazan R, Engelberg-Kulka H (2004) *Escherichia coli* mazEF-mediated cell death as a defense mechanism that inhibits the spread of phage P1. Mol Genet Genom 272:227–234

He W, Huang T, Tang Y, Liu YH, Wu XL, Chen S, Chan W, Wang YJ, Liu XY, Chen S, Wang LR (2015) Regulation of DNA phosphorothioate modification in *Salmonella enterica* by DndB. Sci Rep 5:12368. https://doi.org/10.1038/srep12368

Jun X, Lupeng L, Minjuan X, Oger P, Fengping W, Jebbar M, Xiang X (2011) Complete genome sequence of the obligate piezophilic hyperthermophilic archaeon *Pyrococcus yayanosii* CH1. J Bacteriol 193:4297–4298

Krupovic M, Gonnet M, Hania WB, Forterre P, Erauso G (2013) Insights into dynamics of mobile genetic elements in hyperthermophilic environments from five new *Thermococcus* plasmids. PLoS One 8:e49044

Landini P, Egli T, Wolf J, Lacour S (2014) *SigmaS*, a major player in the response to environmental stresses in *Escherichia coli*: role, regulation and mechanisms of promoter recognition. Environ Microbiol Rep 6:1–13

Li X, Fu L, Li Z, Ma X, Xiao X, Xu J (2015) Genetic tools for the piezophilic hyperthermophilic archaeon *Pyrococcus yayanosii*. Extremophiles 19:59–67

Li P, Tai C, Deng ZX, Gan JH, Oggioni MR, Ou HY (2016a) Identification and characterization of chromosomal relBE toxin–antitoxin locus in *Streptomyces cattleya* DSM46488. Sci Rep 6:32047

Li Z, Li X, Xiao X, Xu J (2016b) An integrative genomic island affects the adaptations of the piezophilic hyperthermophilic archaeon *Pyrococcus yayanosii* to high temperature and high hydrostatic pressure. Front Microbiol 7:1927

Makarova KS, Wolf YI, Koonin EV (2013) Comparative genomics of defense systems in archaea and bacteria. Nucleic Acids Res 41:4360–4377

Masuda H, Tan Q, Awano N, Wu KP, Inouye M (2012a) YeeU enhances the bundling of cytoskeletal polymers of MreB and FtsZ, antagonizing the CbtA (YeeV) toxicity in *Escherichia coli*. Mol Microbiol 84:979–989

Masuda H, Tan Q, Awano N, Yamaguchi Y, Inouye M (2012b) A novel membrane-bound toxin for cell division, CptA (YgfX), inhibits polymerization of cytoskeleton proteins, FtsZ and MreB, in *Escherichia coli*. FEMS Microbiol Lett 328:174–181

Michoud G, Jebbar M (2016) High hydrostatic pressure adaptive strategies in an obligate piezophile *Pyrococcus yayanosii*. Sci Rep 6:27289

O'Connor L, Tangney M, Fitzgerald GF (1999) Expression, regulation, and mode of action of the AbiG abortive infection system of *Lactococcus lactis* sub sp. cremoris UC653. Appl Environ Microbiol 65:330–335

Otsuka Y, Yonesaki T (2012) Dmd of bacteriophage T4 functions as an antitoxin against *Escherichia coli* LsoA and RnlA toxins. Mol Microbiol 83:669–681

Page R, Peti W (2016) Toxin–antitoxin systems in bacterial growth arrest and persistence. Nat Chem Biol 12:208–214

Pecota DC, Wood TK (1996) Exclusion of T4 phage by the *hok*/*sok* killer locus from plasmid R1. J Bacteriol 178:2044–2050

Ramisetty BCM, Santhosh RS (2017) Endoribonuclease type II toxin–antitoxin systems: functional or selfish? Microbiology 163:931–939

Rolfe MD, Rice CJ, Lucchini S, Pin C, Thompson A, Cameron ADS, Alston M, Stringer MF, Betts RP, Baranyi J, Peck MW, Hinton JCD (2012) Lag phase is a distinct growth phase that prepares bacteria for exponential growth and involves transient metal accumulation. J Bacteriol 194:686–701

Schuster CF, Bertram R (2013) Toxin–antitoxin systems are ubiquitous and versatile modulators of prokaryotic cell fate. FEMS Microbiol Lett 340:73–85

Shao YC, Harrison EM, Bi DX, Tai C, He XY, Ou HY, Rajakumar K, Deng ZX (2011) TADB: a web-based resource for Type 2 toxin–antitoxin loci in bacteria and archaea. Nucleic Acids Res 39:D606–D611

Simonato F, Campanaro S, Lauro FM, Vezzi A, D'Angelo M, Vitulo N, Valle G, Bartlett DH (2006) Piezophilic adaptation: a genomic point of view. J Biotechnol 126:11–25

Tachdjian S, Kelly RM (2006) Dynamic metabolic adjustments and genome plasticity are implicated in the heat shock response of the extremely thermoacidophilic archaeon *Sulfolobus solfataricus*. J Bacteriol 188:4553–4559

Tan Q, Awano N, Inouye M (2011) YeeV is an *Escherichia coli* toxin that inhibits cell division by targeting the cytoskeleton proteins, FtsZ and MreB. Mol Microbiol 79:109–118

Tangney M, Fitzgerald GF (2002) AbiA, a lactococcal abortive infection mechanism functioning in *Streptococcus thermophilus*. Appl Environ Microbiol 68:6388–6391

Unterholzner SJ, Poppenberger B, Rozhon W (2013) Toxin–antitoxin systems: biology, identification, and application. Mob Genet Elem 3:e26219

Wang XX, Wood TK (2011) Toxin–antitoxin systems influence biofilm and persister cell formation and the general stress response. Appl Environ Microbiol 77:5577–5583

Wang X, Kim Y, Hong SH, Ma Q, Brown BL, Pu M, Tarone AM, Benedik MJ, Peti W, Page R, Wood TK (2011) Antitoxin MqsA helps mediate the bacterial general stress response. Nat Chem Biol 7:359–366

Winther KS, Gerdes K (2011) Enteric virulence associated protein VapC inhibits translation by cleavage of initiator tRNA. Proc Natl Acad Sci USA 108:7403–7407

Wozniak RA, Waldor MK (2009) A toxin–antitoxin system promotes the maintenance of an integrative conjugative element. PLoS Genet 5:e1000439

Yamaguchi Y, Park JH, Inouye M (2011) Toxin–antitoxin systems in bacteria and archaea. Annu Rev Genet 45:61–79

Zeng X, Birrien JL, Fouquet Y, Cherkashov G, Jebbar M, Querellou J, Oger P, Cambon-Bonavita MA, Xiao X, Prieur D (2009) *Pyrococcus* CH1, an obligate piezophilic hyperthermophile: extending the upper pressure-temperature limits for life. ISME J 3:873–876